Drought Estimation Maps by Means of Multidate Landsat Fused Images

Diego RENZA, Estíbaliz MARTINEZ, Agueda ARQUERO, and Javier SANCHEZ
Department of Architecture and Technology of Computer Systems.
Polytechnic University of Madrid (Spain). Campus de Montegancedo,
28660 Boadilla del Monte, Madrid, Spain

Abstract. The purpose of this paper is to analyze the usefulness of traditional indexes, such as NDVI and NDWI along with a recently proposed index (NDDI) using merged data for multiple dates, with the aim of obtaining drought data to facilitate the analysis for government premises. In this study we have used Landsat 7 ETM+ data for the month of June (2001-2009), which merged to get bands with twice the resolution. The three previous indices were calculated from these new bands, getting in turn drought maps that can enhance the effectiveness of decision making.

Keywords. Drought maps, fused images, NDDI

Introduction

There are two types of natural phenomena related to variables such as rainfall, soil moisture, groundwater, among other: the aridity and drought. Drought is a temporary aberration and it differs from aridity, which is a permanent feature of climate. Although there is not a precise and universally accepted definition of drought, since this phenomenon responds to the particular characteristics of a region and its effects can vary greatly from region to region, a common definition can be found in [1]: "Drought is an insidious natural hazard characterized by lower than expected or lower than normal precipitation that, when extended over a season or longer period of time, is insufficient to meet the demands of human activities and the environment".

The phenomenon of drought occurs in most countries, both dry and wet regions. The impacts are complex, involving many people, varying in spatial and temporal scales that can cause land degradation and, if unchecked, a progression of dry land or an increase in desertification. Drought by itself is not a disaster. Whether it becomes a disaster depends on its impact on local people, economies and the environment and their ability to cope with and recover from it [1,2].

Owing to the creeping nature of drought, its effects often take weeks or months to appear. Precipitation deficits generally appear initially as a deficiency in soil water; therefore, agriculture is often the first sector to be affected. The complexity of the phenomenon of drought hinders the full knowledge of its effects, therefore, is important to monitor and analyze the potential impact of drought in order to identify areas that are most vulnerable to drought [3].

To measure the drought, three main physical ways have been identified, meteorological, agricultural and hydrological. Meteorological drought is defined by a precipitation deficiency threshold over a predetermined period of time; agricultural drought occurs when soil moisture is not sufficient to meet the needs of a particular crop at a critical time and hydrological drought refers to deficiencies in the provision of surface water and groundwater [1]. Droughts are characterized by their duration, intensity and spatial extent; a quantitative assessment of droughts can be estimated deriving statistical properties of historical data on precipitation and other relevant variables such as soil moisture data by using different indices.

The main objective of this study was to obtain drought maps from medium spatial resolution images. These images were fused for enhance spatial resolution and to monitor drought conditions we used the fundamental physical properties relating to wavelength measurements in the visible (red), near infrared and short wave infrared, i.e. *NDVI* (Normalized Difference Vegetation Index), *NDWI* (Normalized Difference Water Index) and *NDDI* (Normalized Difference Drought Index).

1. Drought indices

The role of drought indices is to translate data available from water supply indicators such as rain, snow, flows and others in an understandable representation, which typically is a single value, more useful than raw data for decision making. Although none of the major indices is inherently superior to others in all circumstances, some indices are more suitable than others for certain uses, according to topography, weather, spatial scales or availability of other parameters (temp, soil moisture, snow accumulation, etc.)[2].

Some examples of the conventional tools for measuring the severity of droughts include: Deciles, Standardized Precipitation Index (*SPI*), Palmer Drought Severity Index (*PDSI*), Surface Water Supply Index (*SWSI*) and Crop Moisture Index; this drought monitoring approaches are based on climatic and meteorological observations [4], which can be limited or incomplete for certain regions; in addition they may also be inaccurate or contain errors (human or machine) as well as they cannot be available in real time. Effectiveness is greatly enhanced if multiple indicators are used to describe drought extension and severity [5], in this respect, data obtained by means earth observations are highly complementary to those collected by in-situ systems. In this sense, remote sensing technology has greatly improved the ability to control and manage natural resources, particularly the vegetation indices derived from satellite data to identify areas affected by drought. The combination of different indicators can provide decision makers with enough information to understand the drought phenomenon and estimate its effect [5].

1.1. Drough indices with remote sensing data

The use of remote sensing data has a number of advantages to examine the effects of drought on vegetation. The information covers the entire territory, the repetition of images provides multitemporal measurements [6] and vegetation indices derived from satellite data allow to identify areas affected by drought and take into account different types of vegetation and environmental conditions.

For the calculation of these indices can use low spatial resolution data from different sensors like the Moderate Resolution Imaging Spectroradiometer (MODIS) or Advanced Very High Resolution Radiometer (AVHRR), carried by a series of the (NOAA) satellites [7,8], but with these low spatial resolution sensors it is difficult to study specific forest types, because the pixel size is often greater than the size of forest stands. At higher resolution more detailed information on the forest canopy can be then extracted, so the slow track changes in vegetation, for example, water shortages due to severe drought and heat, can benefit from both satellite images of low and medium resolution for monitoring vegetation and development of forest canopy [9].

Therefore, for a local analysis can be thought of data with greater spatial resolution, as provided by the sensor Landsat 7 ETM+. In this case we have the necessary bands in the red and infrared spectrum to facilitate the calculation of indices. Also the analysis can be further facilitated with fused data, which can be obtained from the original Landsat bands obtaining new bands with twice spatial resolution.

A recent index, *NDDI*, can offer us an appropriate measure of the dryness of a particular area, because it combines information on both vegetation and water, i.e., *NDDI* combines information

776

from the *NDVI* [10] and *NDWI* [11] data. *NDDI* had a stronger response to summer drought conditions than a simple difference between *NDVI* and *NDWI*, and is therefore a more sensitive indicator of drought in grasslands than *NDVI* alone [7].

2. Study area and available data

The Landsat data archive at the U.S. Geological Survey (USGS) Earth Resources Observation and Science (EROS) Center holds an unequaled 36-year record of the Earth's surface and is available at no cost to users via the Internet. Users can access and search the Landsat data archive via the EarthExplorer (EE)1 2 or Global Visualization Viewer (GloVis)2 3 web sites [12].

Landsat Enhanced Thematic Mapper plus (ETM+) multispectral (MS) and panchromatic (PAN) images were used in this study. The images have a spatial resolution of 30 m and 15 m respectively. A subset, 132 km^2 in area, was extracted from scene 201/32 acquired on June (2001-2009, except 2003 due to Scan Line Corrector failure in the ETM+). The upper left corner of the subset is placed at 436507.5 E and 4522312.5 N (UTM geographic coordinates, ZONE 30) for the community of Madrid (Spain), which contains areas of Mediterranean forest, water bodies and urban areas. For the year 2005, the whole image was used for *NDDI* calculation.

For this study, Landsat data for years 2001-2002 and 2004-2009 were selected. The month chosen was June, since it's preceded by good rates of precipitation and average temperatures followed by months with higher temperatures and low rainfall. Climatic data (temperature and precipitation) characteristic of this zone are shown in Figure 1.
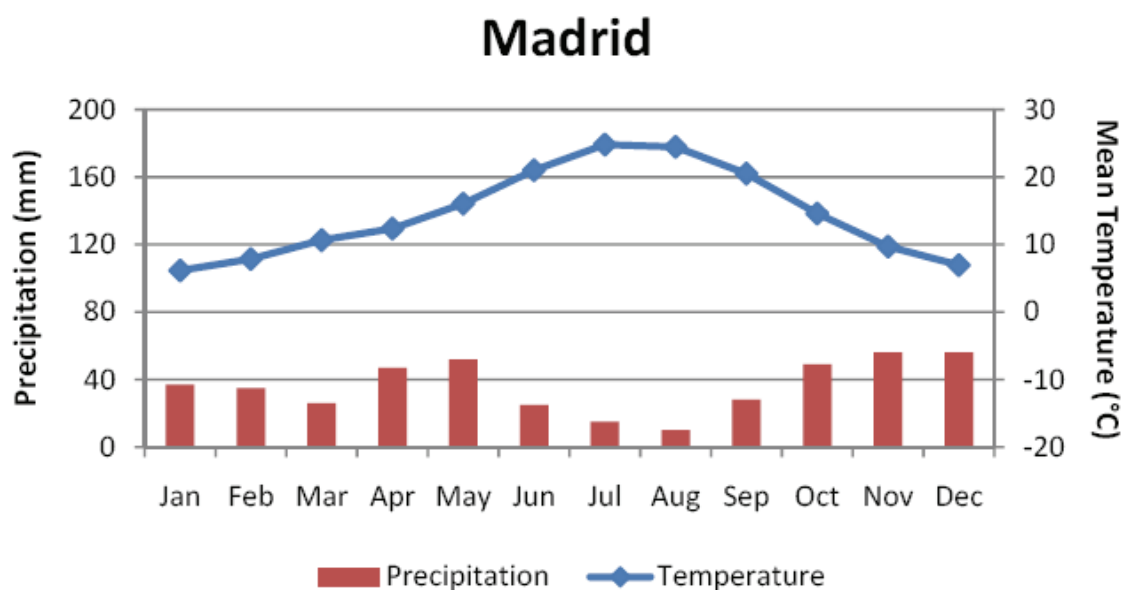
Figure 1: Madrid -Average Temperatures and Precipitation 1971-2000.

3. Methodology

The images used to get drought maps include a PAN image and seven MS bands, therefore the first step was the merging of these images with the aim to exploit both the spatial information contained in PAN as the spectral information contained in the remaining bands. As we worked with a multi-temporal remote sensing images, the fused images was converted to physical units (radiance and

---

[1] http://earthexplorer.usgs.gov
[2] http://glovis.usgs.gov

reflectance) also needed to calculate indices (*NDVI, NDWI, NDDI*). Finally *NDDI* images in grayscale were converted to a drought color scale. The steps developed in this study for each year (month) were:

1. Fusion process: merge images through Dual Tree Complex Wavelet transform (DT-CWT). MS bands were merged with the panchromatic band, getting new bands with a resolution of 15 meters (m). The fusion process applied are summarized in [13]:.

   (a) Radiometric correction and resample the MS image so that their bands have the same pixel size as the PAN image.

   (b) These bands, along with the PAN are decomposed by means of DT-CWT.

   (c) Preserve MS Approximation.

   (d) The PAN detail coefficients are compared with the respective MS coefficients and the highest are used as they describe the high frequency component.

   (e) Computation of inverse DT-CWT to these new coefficients.

2. Reflectance calculation: Radiometric calibration and reflectance conversion. With the Level 1 Landsat products the users receive the information as calibrated Digital Numbers (DNs) representing each pixel. To calculate the above indices is necessary to convert DNs to physical units. For this we have applied the equations and factors outlined in [12].

3. *NDVI* and *NDWI* calculation. With the reflectance values, we calculated the *NDVI* and *NDWI* according to Eq. (1) and (2),

$$NDVI = \frac{\rho_{NIR} - \rho_{RED}}{\rho_{NIR} + \rho_{RED}} \tag{1}$$

$$NDWI = \frac{\rho_{NIR} - \rho_{SWIR}}{\rho_{NIR} + \rho_{SWIR}} \tag{2}$$

   where ρ_{NIR} is there flectance in the near infrared channel (0.78-0.90 μm Landsat TM/ETM+), ρ_{RED} is the reflectance in the visible channel (0.63-0.69 μm Landsat TM/ETM+) and ρ_{SWIR} is the reflectance in the mid-infrared channel(1.55-1.75 μm Landsat TM/ETM+).

4. *NDDI* calculation. Since the *NDVI* and *NDWI* varies in a range from -1 to +1, for the calculation of *NDDI* these values were converted to 8 bits (0-255), therefore *NDDI* ranges between -1 and +1. The *NDDI* [7] was calculated according to the Eq. (3),

$$NDDI = \frac{NDVI - NDWI}{NDVI + NDWI} \tag{3}$$

   Comparing *NDDI* we used two additional indices, *NDVI$_{DEV}$* : *NDVI* Deviation index [2], and *VCI*: Vegetation Condition Index [10]:

$$NDVI_{DEV} = NDVI_i - NDWI_{mean,m} \tag{4}$$

$$VCI = \frac{NDVI - NDWI_{MIN}}{NDVIMAX - NDWI} \tag{5}$$

5. Use of colour tables in *NDDI* images. With the *NDDI* calculated, drought maps were generated according to the scales showed in Figure 3 (i). It is important to note that the scale may vary according to the characteristics of an area.

4. Results

Figure 2 shows the average in each of the years studied for five different indices: *NDVI, NDVI, NDDI, NDVI$_{DEV}$* and *VCI*. First, we can see that the shape of *NDVI* and *NDWI* is quite similar, hence its normalized difference tends to remain constant, which is precisely reflected by the *NDDI*. In the event that one of these two values to distance itself from the other, cause a deviation from the trend, which in turn causes the *NDDI* increase or decrease. This is particularly noticeable in 2005, which in turn have been one of the driest years in recent years [14].

778

In the case of *VCI* one can see that its shape is similar to the one of other indices. According to this index the driest year was 2005 (in agreement with *NDDI*), in which the index falls below the average. Also the wetter years according to this index were 2006, 2007 and 2008. It should be noted here that this index takes as reference the minimum and maximum values of *NDVI* for a time series. In the case of $NDVI_{DEV}$ its shape is quite similar to that provided by the NDVI with the characteristic that has a vertical displacement caused by the subtraction of the average value of the series.
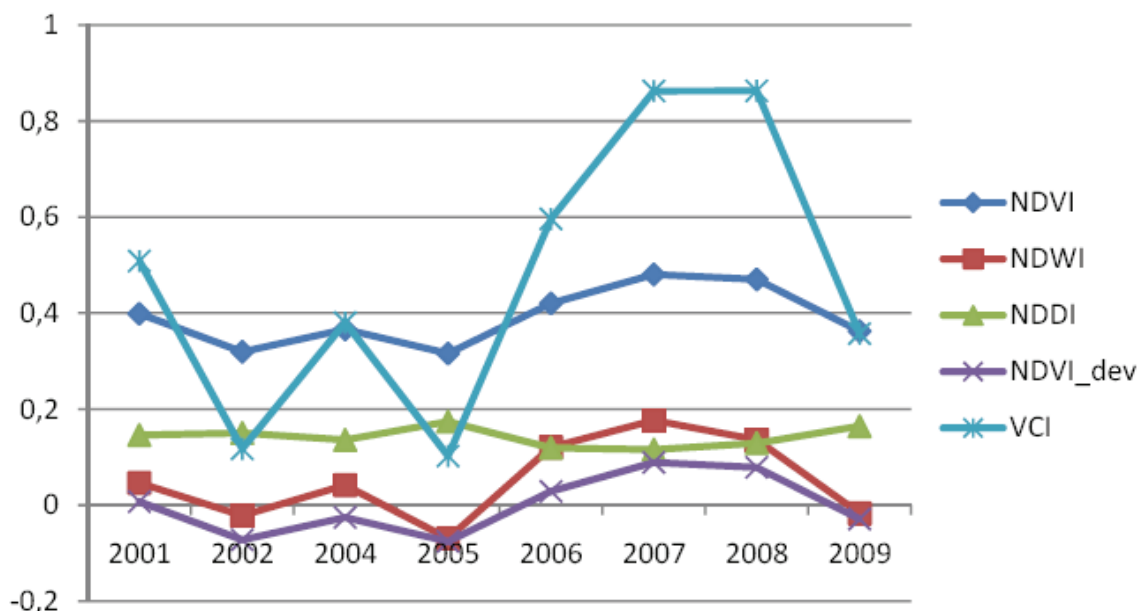
Figure 2. Average drought indices obtained: *NDVI, NDWI, NDDI, NDVI_{DEV}* and *VCI* in June for eight Years (2001-2009, except 2003)

Figures 3(a-h) show the drought maps for each of the years studied, at a glance the comparison within an entire area for a multi-temporal series it's straightforward. In this case we can conclude that 2005 image shows highest deficiencies in the provision of surface water and highest drought values.

As mentioned above $NDVI_{DEV}$ and *VCI* indices make use of data collected from a multi-temporal series, including the maximum, minimum and average. These parameters can vary greatly depending on the size of the series. In the case of *NDDI*, the values obtained are independent of both the size of the study area as of the time series. The maps shown in the Figure 3 correspond to an area of 132 km^2, however, if it is greater area, as shown in Figure 4(a), after performing the process and select the same area will reach the same result. This is illustrated in Figure 4, which is a zone of 22500 km^2; the location of the study area is highlighted too.

The average of the indices shown in Figure 2 has been calculated for a small area, in which case you may receive an approximate idea of changes that have each of the indices over the time series. By taking a wider region, as shown in Figure 4(a), by plotting the averages of each year, his profile would be flatter than the responses shown in Figure 2 which in turn may make it less easy to interpret and analyze the effects of drought.

Therefore, for local impact studies, when you have images of higher spatial resolution, both the spectral index calculation and graphical representation gives a more accurate picture of the behavior that has had a particular area over time. In the case of Landsat 7 PAN and MS information can be combined to obtain a product that takes advantage of those characteristics. This is the main reason for the use of images with greater spatial resolution.

Indeed, with Figure 4 we can appreciate the benefits of having a medium resolution to generate drought maps. For its part the Figure 4(a) provides an overview of a large area, while Figure 4(b) allows us to appreciate further a particular area.
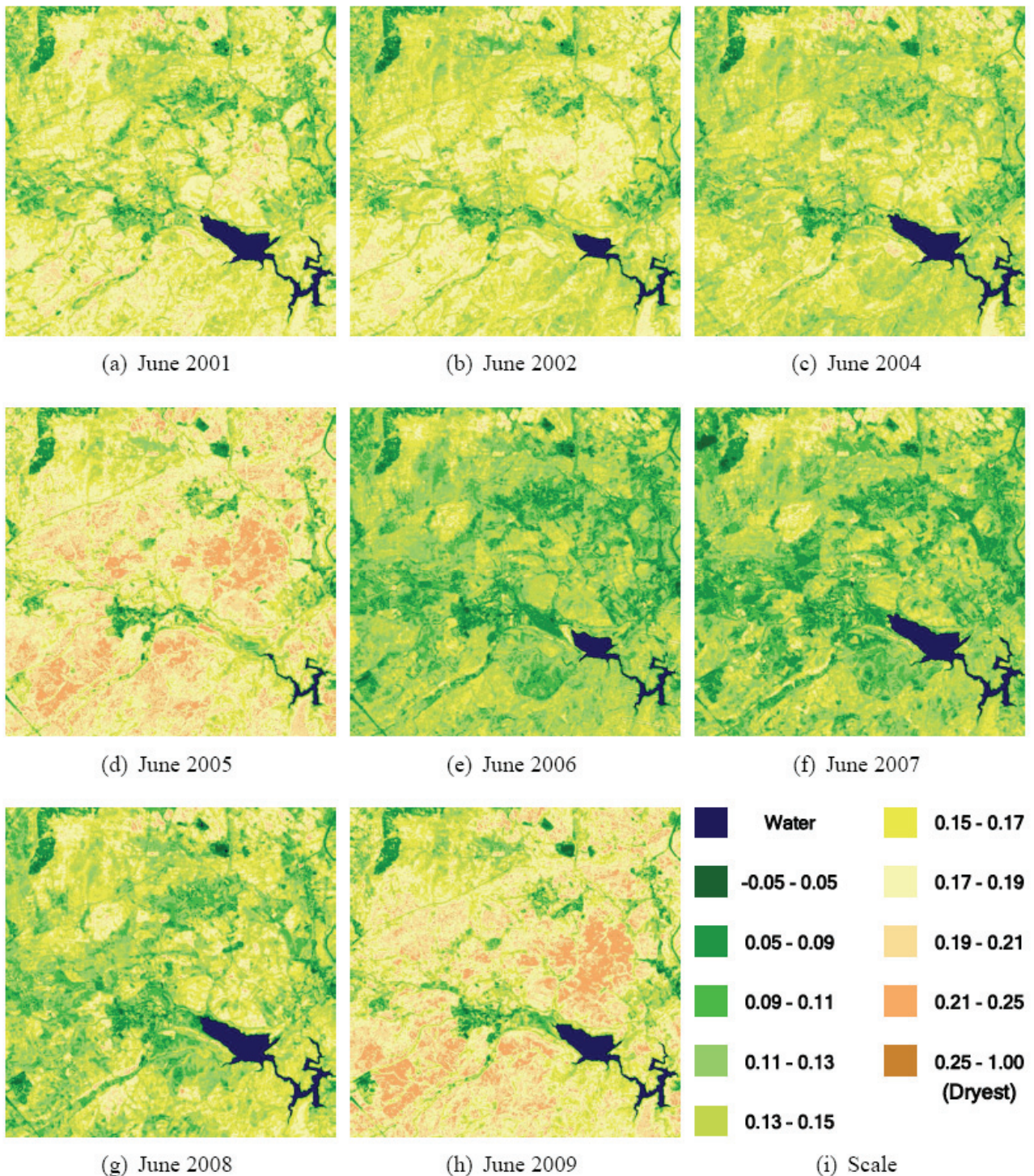
Figure 3. Drought maps obtained from NDDI corresponding to June for eight Years (2001-2009, except 2003)
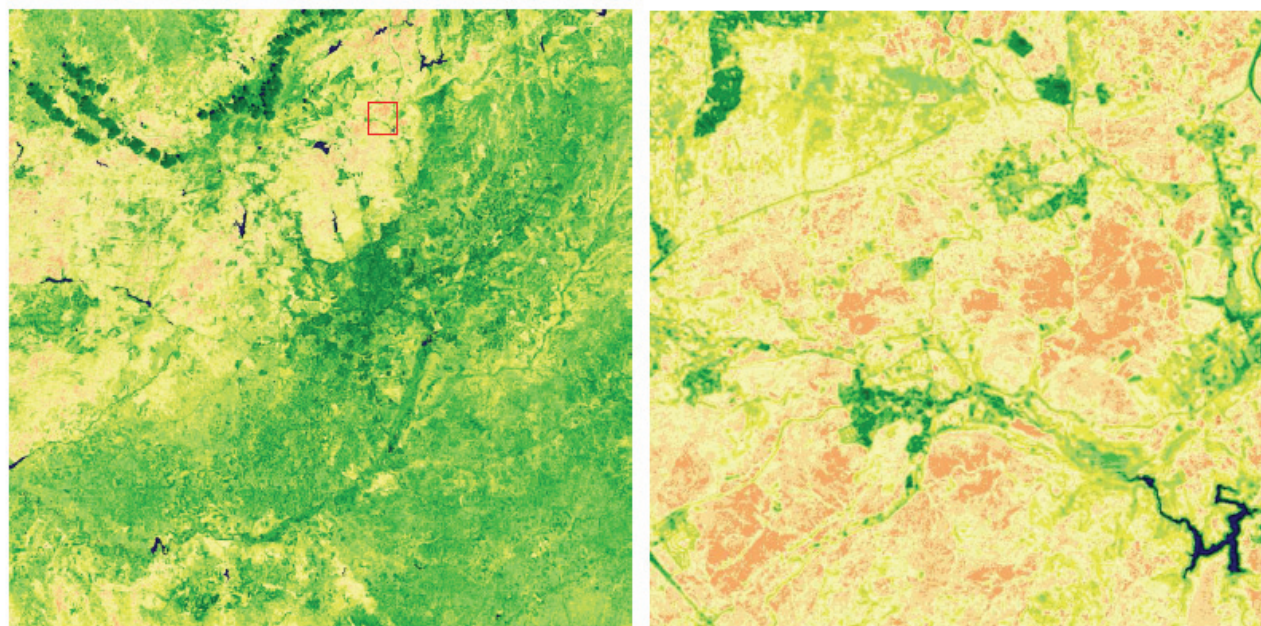
(a) Wider scene - 22500 km^2 (b) Smaller scene - 132 km^2

Figure 4. Drought maps obtained from NDDI corresponding to June 2005 for two different areas

5. Conclusions

The use of remote sensing data in the study of natural phenomena facilitates the implementation of indicators that allow a clear view of the whole area, enabling graphically assess a particular factor in an area in relation to its environment. This will benefit both areas associated with decision making and environmental impact assessment.

The NDDI is characterized by its ease of calculation because it is based on normalized difference (addition and subtraction) and it does not depend on time series data. It is important to note that this index can be an optimal complement to in-situ based indicators or for other indicators based on remote sensing data.

The benefits of higher spatial resolution directly related to the images used and improved by fusion processes can be an alternative in the study of drought in areas that depend on small local governments, in relation to this last is necessary to take into account the temporal resolution of the data required for a given study.

References

[1] *Drought monitoring and early warning: concepts, progress and future challenges*, World Meteorological Organization, WMO No. 1006, 2006.

[2] R. Magno, Drought definitions indexes and mapping, Mediterranean Training seminar, Florence - Italy, July 2006.

[3] T. Tadesse, Drought Indices: Overview and application, Mediterranean Training seminar, Florence - Italy, July 2006.

[4] A. Ghulam, Q Qiming, T. Teyip; Z.L. LI, Modified perpendicular drought index (MPDI) : a real-time drought monitoring method, ISPRS journal of photogrammetry and remote sensing, Vol. 62, No. 2, pp. 150-164, 2007.

[5] L. Garrote, F. Martin-Carrasco, F. Flores-Montoya, A. Iglesias, Linking drought indicators to policy actions in the tagus basin drought management plan, Water resources management, Vol. 21, No 5, pp. 873-882, 2007.

[6] S.M. Vicente-Serrano, Evaluating the impact of drought using remote sensing in a Mediterranean, semi-arid region, Natural Hazards 40, pp. 173-208, 2007.

[7] Y. Gu, J.F. Brown, J.P. Verdin, B. Wardlow, A five-year analysis of MODIS NDVI and NDWI for grass-land drought assessment over the central Great Plains of the United States, Geophys. Res. Lett., Vol. 34, 2007.

[8] P.S. Thenkabail, M.S. Gamage, V.U. Smakhín, The Use of Remote Sensing Data for Drought Assessment and Monitoring in Southeast Asia. Research Report 85. IWMI. Colombo-Sri Lanka, Intemational Water management Institute, 2004.

[9] M. Deshayes, G. Guyon, H. Jeanjean, N. Stach, A. Jolly, O. Hagolle, The contribution of remote sensing to the assessment of drought effects in forest ecosystems, Annals of Forest Science, 63, 6, pp. 579-595, 2006.

[10] R.P. Singh, S. Roy, F. Kogan, Vegetation and temperature condition indices from NOAA AVHRR data for drought monitoring over India. Int. Journal of Remote Sensing, Vol. 24, 22, pp. 4393 - 4402, 2003.

[11] T.J. Jackson, D. Chen, M. Cosh, L. F. Li, M. Anderson, C. Walthall, P. Doriaswamy, E. Hunt, Vegeta-tion water content mapping using landsat data derived normalized difference water index for corn and soybeans, Remote sensing of environment, 92, pp. 475-482, 2004.

[12] G. Chander,B.L. Markham, D.L. Helder, Summary of Current Radiometric Calibration Coefficients for Landsat MSS, TM, ETM+, and EO-1 ALI Sensors. Remote Sensing of Environment, Vol. 113, 5, 2009.

[13] D. Renza, E. Martinez, A. Arquero, Optimizing classification accuracy of remotely sensed imagery with DT-CWT fused images, 14th Iberoamerican Congress on Pattern Recognition, CIARP 2009 LNCS, Guadalajara, Mexico, 2009.

[14] http://earthobservatory.nasa.gov/NaturalHazards/view.php?id=14719 (Accessed May 10, 2010)